

Self-Regenerating of Functional Polymer Surfaces by Triggered Layer Shedding Using a Stimulus-Responsive Poly(urethane)

Zhuoling Deng and Karen Lienkamp*

Regeneration of functional surfaces after damage or contamination could extend the life time of devices. Such regeneration can be achieved by layer shedding (like a lizard shedding its skin). In this work, triggered self-regeneration of functional surfaces by an external stimulus is presented. Polymer multilayer stacks are assembled alternately from discrete 20–300 nm thick functional layers and depolymerizable interlayers, which are used as sacrificial layers. The sacrificial layers are depolymerizable poly(benzyl carbamates) end-capped with 4-hydroxy-2-butanone. Their depolymerization is triggered by alkaline pH, at which the end-cap is cleaved. This initiates a 1,6-elimination cascade of the polymer backbone, during which CO₂ is released. Thus, the layer shedding is driven synergistically by mass transport and buoyancy forces. Proof-of-concept is achieved using poly(styrene) as a model functional layer, and also studied for hydrophilic, antimicrobially active poly(oxanorbornene) layers. The multilayer assembly and disassembly process is monitored by ellipsometry, Fourier transform infrared spectroscopy (FTIR), optical microscopy, and atomic force microscopy. FTIR spectra taken after degradation are confirmed the regeneration of the surface functionality.

coatings. A representative example for the latter are polymer-based anticorrosion coatings on metals. These find applications in aerospace engineering, microelectronics, packaging, as well as the biomedical industry.^[1] Recent work on polymeric anticorrosion coatings focuses on identifying and characterizing the failure mechanism at such interfaces on the molecular level, and on strategies to enhance the coating durability,^[2] for example, for use in a maritime environment.^[3]

Damages at interfaces are often induced by property mismatches of the materials involved, e.g., by a mismatch of their thermal expansion coefficients, Young's moduli, or Poisson ratios. When changes in environmental conditions (for example, in temperature or humidity) cause significantly different property responses, adjacent layers often buckle at the interface, leading to mechanical failure.^[4] In many industries including aeronautics, composites that do

not have the required dimensional stability to prevent such delamination cannot be used.^[5]

There are two different scenarios for failure at interfaces: In cohesive failure, an interlayer between two adjacent materials is disintegrated, i.e., the cohesive forces between the interlayer components are overcome by an external event. This is the case when two materials glued together are pulled apart, and the break line goes through the glue phase. The other scenario is adhesive failure. In the above example of the glued materials, the glue layer would separate as a whole from one of the adjacent materials, i.e., the break line is located at the glue-material interface. Whether adhesive or cohesive failure takes place depends on the relative energies of cohesion and adhesion of the system.

In systems where delamination is a desired event, either the energy of adhesion or of cohesion needs to be altered. Examples for such systems are molting reptiles and crustacean in nature, cell sheet detachment from a cell culture dish in tissue engineering, sacrificial layers used in microsystem engineering, or the disassembly of layer-by-layer systems.^[6] The epidermal renewal of reptiles is a cyclic process with simultaneous formation of new skin layers under the old skin layer. An in-between layer is degraded to facilitate the shedding of the old skin.^[6a] This detachment is assisted by external mechanical forces, e.g., when a snake rubs between stones during molting.^[6b] In tissue engineering, cell sheet detachment from culture dishes can


1. Introduction

Solid materials with interfaces to polymers are abundant and comprise polymer composites, laminates, blends, and polymeric

Z. Deng, K. Lienkamp
 Department of Microsystems Engineering (IMTEK)
 University of Freiburg
 Georges-Köhler-Allee 105, Freiburg 79110, Germany
 E-mail: karen.lienkamp@uni-saarland.de

Z. Deng, K. Lienkamp
 Freiburg Center for Interactive Materials and Bioinspired Technologies (FIT)
 University of Freiburg
 Georges-Köhler-Allee 105, Freiburg 79110, Germany

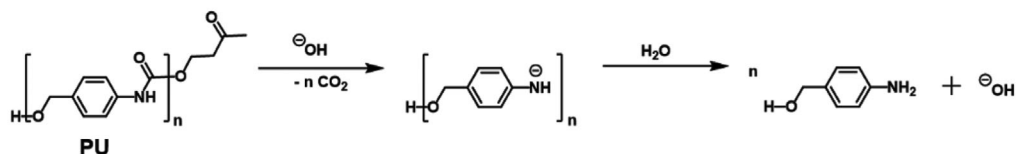
K. Lienkamp
 Institut für Materialwissenschaft und Werkstoffkunde
 Universität des Saarlandes
 Campus, Saarbrücken 66123, Germany

 The ORCID identification number(s) for the author(s) of this article can be found under <https://doi.org/10.1002/macp.202100127>

© 2021 The Authors. Macromolecular Chemistry and Physics published by Wiley-VCH GmbH. This is an open access article under the terms of the Creative Commons Attribution License, which permits use, distribution and reproduction in any medium, provided the original work is properly cited.

DOI: 10.1002/macp.202100127

a) Depolymerization of poly(benzyl carbamate):



b) Different end groups of poly(benzyl carbamate):

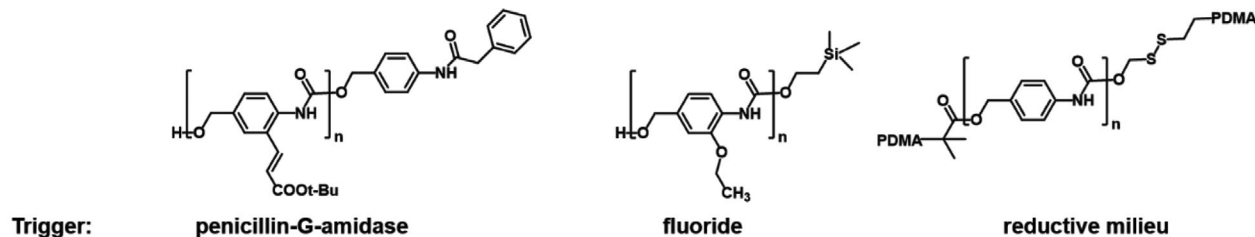


Figure 1. a) Structure of a poly(benzyl carbamate) with a 4-hydroxy-2-butanonyl end group (PU), and mechanism of depolymerization of under alkaline trigger conditions; b) Poly(benzyl carbamates) with different end groups susceptible to various triggers: a benzyl amide end group that can be cleaved by penicillin-G-amidase, a trimethylsilyl end group removable by fluoride, and a disulfide end group that is cleavable by reduction (PDMA = poly(*N,N*-dimethylacrylamide)).

be triggered by thermo-responsive poly(*n*-isopropylacrylamide) (PNIPAM), which undergoes a conformational transition at its lower critical solution temperature (LCST). When cells are cultured on PNIPAM, changing the temperature below the LCST disturbs the cell adhesion at the PNIPAM-cell interface, and the mature cell sheet can peel off as an intact sheet without previous enzymatic degradation.^[6c-g] Another example of desired delamination events are ultrathin polyelectrolyte multilayers obtained by the layer-by-layer (LbL) method, which can be disassembled using electrochemical triggers, pH-triggers, or changes in the ionic strength. These affect the polyelectrolyte charge and thus either weaken the interphase cohesion or interface adhesion.^[6h,7,8]

In these systems, a mismatch of certain material properties in response to external conditions is deliberately sought to induce buckling and delamination. On the microscopic or molecular level, this can be caused by different processes, e.g., conformational changes of molecules, or changes of the interfacial properties. Additional external mechanical forces can then help to break the connection between the different layers.

In our group, we developed a sacrificial layer approach for intentional delamination of polymer layers from multilayer stacks. Instead of thin LbL systems, we are working with discrete, relatively thick layers (20–300 nm). These resemble a nanoscale stack of pancakes, unlike the LbL architectures which are more like scrambled eggs. These stacks consist of alternatingly applied functional layers and sacrificial layers. By disintegration of the sacrificial layer, the functional layer on top of it is intentionally delaminated, and a new functional layer further down the layer stack is uncovered. Thus, the function of the material could be regenerated after contamination or damage of the top layer—like a lizard shedding its skin. In one previously reported system, an interlayer made from poly(sebacic acid anhydride) (PSA) positioned between two polymer networks made from antimicrobial poly(oxanorbornenes) was degraded under acidic conditions and shed the top layer to regenerate the antimicrobial functionality.^[9]

Other studies with PSA, poly(adipic anhydride), or poly(salicylic acid-*co*-sebacic acid) demonstrated that the degradation kinetics are key for a success of this process.^[10] If the process is too slow the loosened top layer has sufficient time to re-form adhesive interactions with the remaining stack, which prevents delamination. With fast disassembly kinetics, for example by the triggered depolymerization of poly(ethyl glyoxylate), delamination was successful.^[10b]

In this work, we explore the potential of another stimulus-responsive polymer to achieve intentional delamination from polymer multilayer stacks, namely poly(benzyl carbamates). These polymers were chosen for two reasons: first, their depolymerization can be triggered, and second, carbon dioxide is released during depolymerization (Figure 1a). We anticipated that when such a layer is depolymerized in a multilayer stack, gas evolution can help to lift the upper functional layer and thereby impede its re-attached to the function layer underneath. Only very recently, oxygen development was used to release micro- and nanofabricated structures from a rigid substrate, and a poly(pyrrole) film was delaminated from carbon electrodes with the help of chlorine gas.^[11] Both studies indicate the feasibility of our concept.

Like poly(ethyl glyoxylate), poly(benzyl carbamate) belongs to the group of self-immolative polymers (SIPs).^[12] SIPs are polymers that can be triggered to disassemble sequentially after a single triggering event by which their stabilizing end group is removed. Some SIPs have a ceiling temperature below the temperature of application and depolymerize head-to-tail when their stabilizing end group is cleaved.^[12] This process can be triggered by UV light, a change in temperature, or a chemical stimulus. Depending on the structure of the polymer backbone and its length, the depolymerization of SIPs can take place in seconds up to minutes.^[13] Thus, SIPs disassembly is faster by at least one order of magnitude than the hydrolysis of degradable poly(anhydrides).^[10a] This increases the mass transport of molecules at the materials interface, which seems

to assist the delamination process. The degradation cascade of poly(benzyl carbamates) is based on a 1,6-elimination process (Figure 1a), which can be triggered by various stimuli depending on the nature of the stabilizing end-group. For example, end groups could be cleaved by penicillin-G-amidase, fluoride, or reduction (Figure 1b).^[12,14] In this work, we used poly(benzyl carbamate) with a 4-hydroxy-2-butanonyl end group (called **PU** in the following) as a sacrificial layer.

2. Results

2.1. Study Design

The aim of this study was to demonstrate triggered delamination of a functional layer from polymer multilayer stacks using the poly(benzyl carbamate) **PU** (Figure 1a) as a sacrificial layer. The triggered depolymerization of **PU** should induce sufficiently fast diffusion of the depolymerization products out of the contact zone of the layers, and thereby enable detachment of the functional layer. This process should be further assisted by CO₂ release during depolymerization (Figure 2a). The synthesis of **PU** by a combination of literature procedures is shown in Figure 2b. We first tested the feasibility of the concept by shedding a polymer layer from a two-layer model system with **PU** as sacrificial layer, and then investigated several two-layer and three-layer systems which contain functional layers with antimicrobial activity. The polymers used, as well as their acronyms, are shown in Figure 2c. Poly(styrene) (**PS**, with co-repeat units carrying the cross-linker benzophenone) was chosen as a model compound because of its hydrophobicity and charge-neutrality. It was cross-linked with benzophenone for additional mechanical stability of the layer. With this, we could establish a proof-of-concept of the combined depolymerization/gas evolution assisted delamination process and demonstrate its efficiency in removing an attached polymer layer in a two-layer system (Figure 2d). We then investigated a two-layer system consisting of a **PU** bottom layer and the antimicrobial polymer poly(guanidium oxanorbornene) (**PGON**, with 10% diazoester cross-linker repeat units), and a three layer system consisting of **PU-PS-PGON** (Figure 2d).^[15] An additional three layer system consisting of functional layers made from the antimicrobial poly(carboxyzwitterion) (**PZI**, also with 10% diazoester cross-linker) and **PU** (**PZI-PU-PZI**, Figure 2d) with varying **PU** layer thickness has also been tested to examine the effect of the sacrificial layer thickness on the system delamination. Unlike **PGON**, which is positively charged, **PZI** is polyzwitterionic.^[16] Thus, its surface charges should interfere less with the delamination process than the surface charge of **PGON**.

The multilayer stacks used for these experiments were assembled by spin-coating using orthogonal solvents for the different layers. The **PS**, **PGON** and **PZI** layers were UV cross-linked to obtain stable hydrogels. The multilayer stacks were studied by ellipsometry, Fourier transform infrared spectroscopy (FTIR), and where applicable also by microscopy and/or atomic force microscopy (AFM)—both before and after the delamination process—to determine their thickness, the presence of functional groups, and to observe morphological changes.

2.2. Polymer Synthesis and Multilayer Studies

2.2.1. Polymer Synthesis

The synthesis of the polyurethane end-capped with 4-hydroxy-2-butanone (**PU**) is shown in Figure 2b, and the details are described in Section 1 (Figures S1–S4) of the Supporting Information. A **PU** with a number average molecular mass (M_n) of 2300 g mol⁻¹ was obtained according to end group analysis by ¹H-NMR; according to gel permeation chromatography, M_n was 3000 g mol⁻¹, with a polydispersity index of 1.3.

Poly(styrene-co-4-methacryloyloxybenzophenone) (**PS**), poly(guanidium oxanorbornene) with diazoester co-repeat units (**PGON**), and the poly(carboxyzwitterion) with diazoester co-repeat units (**PZI**) were synthesized as reported previously.^[15–17]

2.2.2. General Considerations for Polymer Multilayer Assembly and Disassembly

The polymer multilayers shown in Figure 2 were assembled on silicon substrates by spin-coating from orthogonal solvents. In this process, the solvent of the layer applied should be a non-solvent for the layers underneath, so that disintegration of these layers is avoided.^[10b] Details of the exact assembly conditions (solvents, polymer concentrations, surface pretreatment, etc.) are given in the Experimental Section and Section 2 of the Supporting Information.

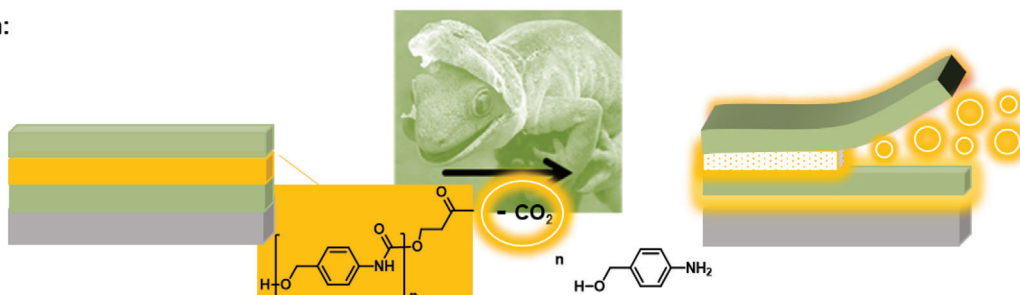
2.2.3. PS-PU Layer System and PGON-PU Layer System

Assembly. The characterization data obtained during the assembly of the **PS-PU** layer system with **PU** as sacrificial layer and **PS** as model functional layer on top is shown in Figure 3a. A thin layer of **PU** with a layer thickness of 21 ± 0.5 nm (determined by ellipsometry) was obtained. The thickness of the resulting **PS-PU** system was 78 ± 0.5 nm, i.e., the **PS** layer had a thickness of about 57 nm. A comparison of the FTIR spectra of the **PS-PU** system and the **PU** layer alone indicated the presence of an additional peak at 1668 cm⁻¹, which can be assigned to the carbonyl group in the diaryl ketone group of the benzophenone cross-linker (blue arrow in Figure 3a).^[18]

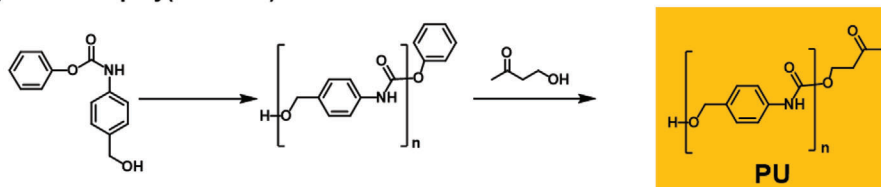
Data obtained from the **PGON-PU** layer system consisting of **PU** as sacrificial layer and **PGON** are shown in Figure 3b. The thickness of the **PU** layer was 14 ± 0.5 nm (from ellipsometry). The thickness of the resulting **PGON-PU** system was 96 ± 3 nm (**PGON** thickness: about 82 nm). In the FTIR spectrum of the **PGON-PU** system, two additional peaks at 1709 and 1674 cm⁻¹ appeared compared to the pure **PU** spectrum, which could be assigned to the imide carbonyl, and the C=N imine of the guanidium group, both of which are components of **PGON** (arrows in Figure 3b).^[18]

Disassembly. NaOH at a concentration of 0.1 mol L⁻¹ was used to trigger depolymerization of **PU**. In previous work, depolymerization of a similar poly(benzyl carbamate) with a 4-hydroxy-2-butanone end group was initiated by bovine serum albumin (BSA) in NaHCO₃ buffer at pH 8.3;^[12,19] however, these reaction conditions did not trigger **PU** depolymerization in our hands. Potential reasons for this are the only partial end-capping of **PU** with

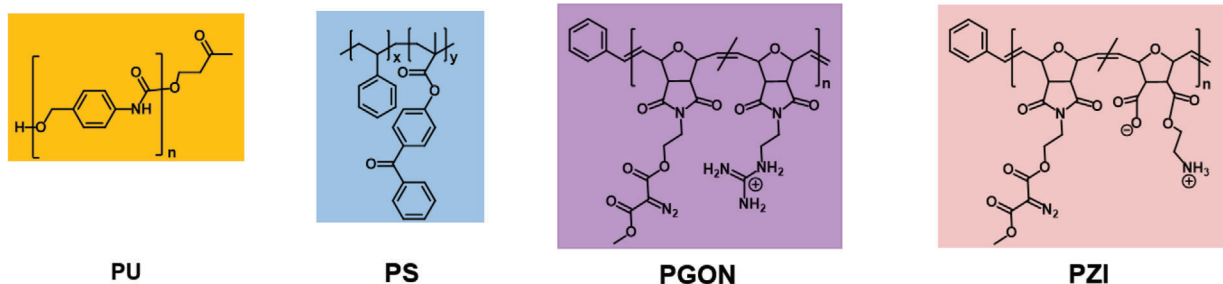
a) Aim:



b) Synthesis of poly(urethane):



c) Polymers used:



d) Material design:

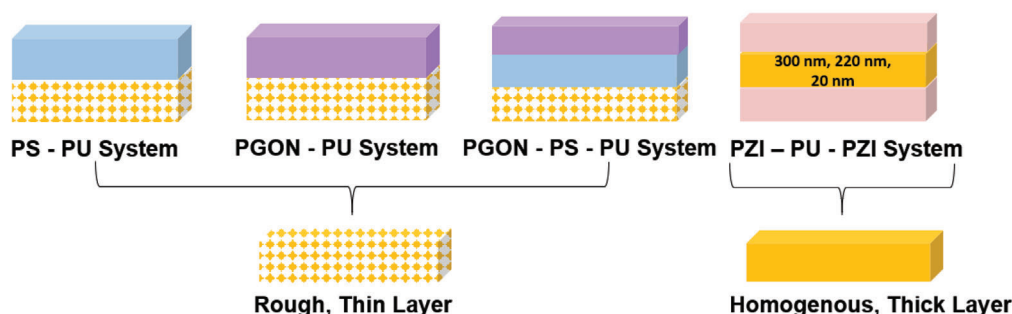


Figure 2. a) The aim of this work was surface regeneration of a functional layer from a polymer multilayer stack. Like a lizard shedding its skin, this was achieved by a combination of a sacrificial layer with mechanical forces. Here the sacrificial layer undergoes triggered depolymerization, which is combined with buoyancy forced due to gas evolution. b) Synthesis of the poly(benzyl carbamate) **PU** with a 2-butanonyl end group; c) Polymers used: poly(benzyl carbamate) **PU**, a UV cross-linkable poly(styrene) with 5% methacryloyl-4-oxy-benzophenone repeat units (**PS**), a UV cross-linkable poly(guanidinium oxanorbornene) (**PGON**) with 10% diazoester cross-linker groups, and a poly(carboxy-zwitterion) (**PZI**), also with 10% diazoester cross-linker repeat units. d) System design: **PS-PU** two layer system consisting of **PU** as sacrificial layer and **PS** as a model functional layer; **PGON-PU** two layer system consisting of **PU** as sacrificial layer and **PGON** as functional layer; **PGON-PS-PU** three layer system made from a **PU** bottom layer, a **PS** interlayer and a **PGON** top layer; **PZI-PU-PZI** three layer systems made from a **PU** interlayer with varying thickness (300, 220, and 20 nm, respectively) between two cross-linked **PZI** layers. The **PU** layer used had different morphologies, the checkered orange layer in the figures refers to a rough, 14–20 nm thin layer; the solid orange layer refers to homogenous and thick layer. Photograph in (a) adapted with permission.^[9] Copyright 2015, American Chemical Society.

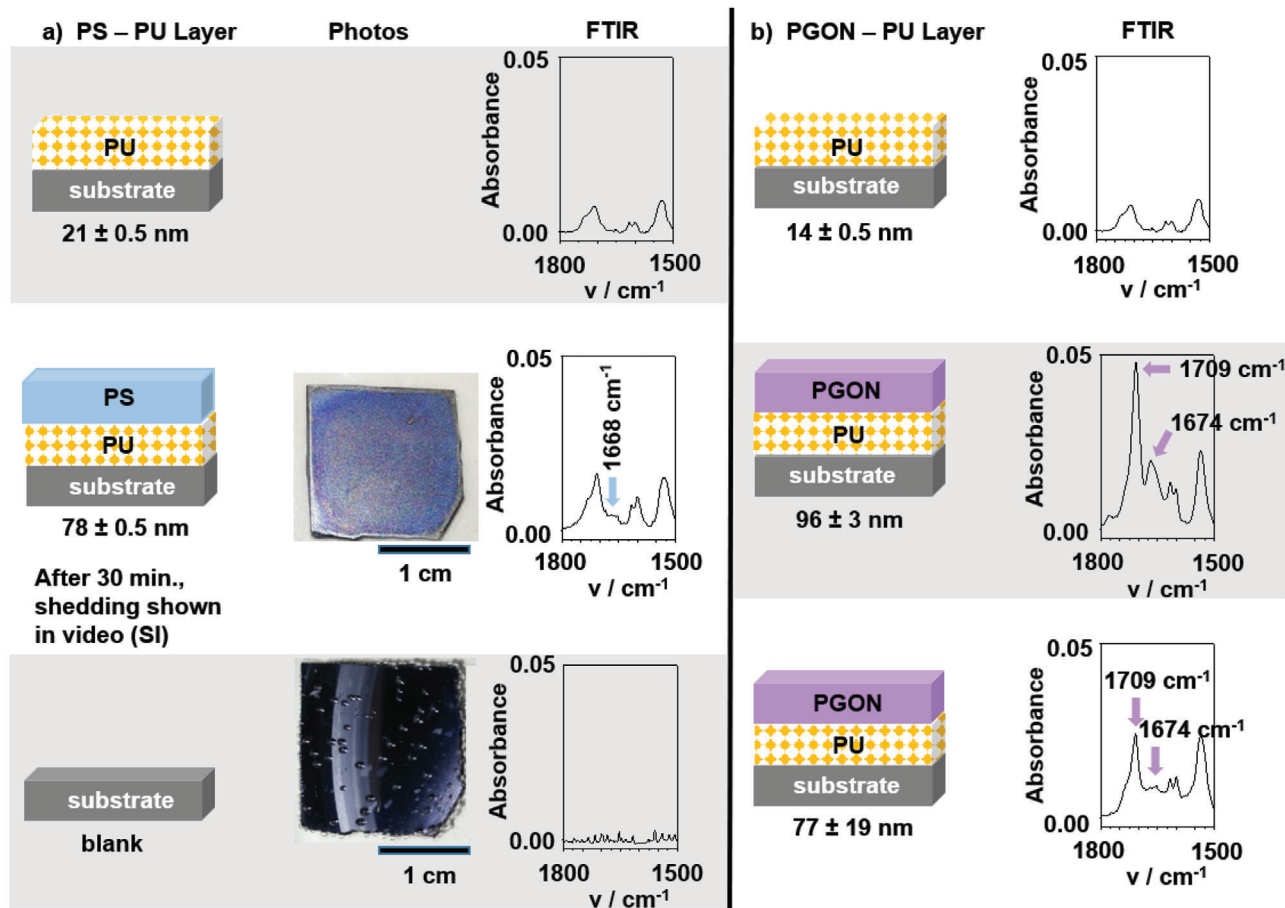


Figure 3. Assembly and disassembly of a) the PS-PU and b) PGON-PU layer systems studied by ellipsometry and FTIR. For the PS-PU system, the CO₂ evolution was documented in photographs and in a video (see Supporting Information).

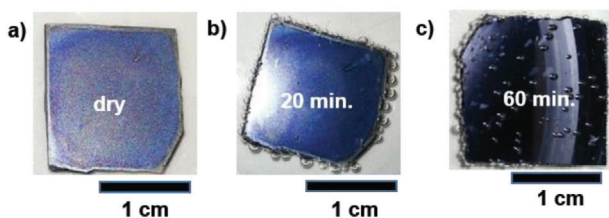


Figure 4. Photographs of the delamination of the A-B system: a) in the dry state, b) after 20 min in NaOH, and c) after 60 min in NaOH.

the BSA-cleavable 2-butanonyl groups (57%, as described in Section 1 of the Supporting Information), and second, the structural variation of PU compared to the poly(benzyl carbamate) used in the literature. The latter had *ortho*-acrylic acid substituents and thus a potentially better solubility in aqueous buffer. Therefore, a stronger base was used for the here presented PU.

For layer shedding, the PS-PU system was immersed in NaOH, and the degradation was documented by photographs (Figure 4). After 20 min, the appearance of gas bubbles on the edges of the sample indicated the onset of depolymerization. Over time, the bubbles grew larger and started to appear all over the sample. After 30 min, the PS layer rolled up from one edge,

was lifted up by buoyancy forces, and was obtained as an intact layer. This process was recorded in a video (Section 3 of the Supporting Information). The entire delamination process took about 60 min, leaving behind a blank substrate (Figure 4c).

Unlike the PS-PU system, the PGON-PU system did not delaminate when immersed into NaOH for 60 min, nor was any gas evolution detected. According to ellipsometry, the thickness of the PGON-PU system stack was only reduced from 96 ± 3 nm to 77 ± 19 nm (the large measurement error of the second value reflects a significant increase of the layer roughness). While all FTIR signals were reduced in intensity after NaOH treatment, the characteristic PGON peaks at 1709 and 1674 cm⁻¹ were still present (Figure 3b). This indicated extraction of the some non-cross-linked parts of the PGON, but no layer shedding.

2.2.4. PGON-PS-PU Layer System

The results of the PS-PU layer and PGON-PU layer systems demonstrated that PU can be used as a sacrificial layer, but that its function seems to be compromised by the presence of PGON, possibly by ionic interactions between polycationic PGON and the negatively charged PU intermediates that form after triggering. These interactions possibly quench the depolymerization

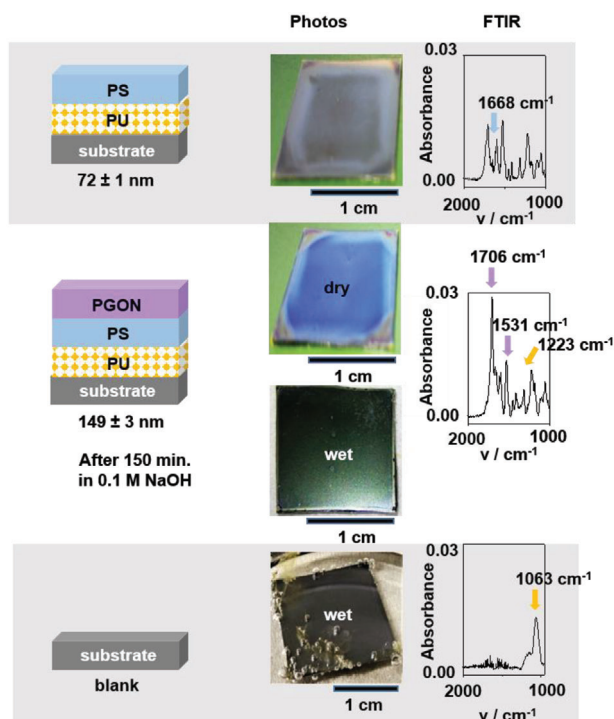


Figure 5. Assembly and disassembly of the PGON-PS-PU system, studied by ellipsometry and FTIR.

cascade. This hypothesis was tested with a PGON-PS-PU three-layer system with an additional PS interlayer, i.e., with no direct contact between PU and PGON.

Assembly. Data taken during the assembly of the PGON-PS-PU three-layer system with a PS interlayer are summarized in Figure 5. The layer thickness of the PU layer was 14 ± 0.4 nm. The PGON-PS bilayer had a total thickness of 72 ± 1 nm, i.e., the PS layer was about 58 nm thick. A characteristic PS layer peak at 1668 cm^{-1} (carbonyl signal of the diaryl ketone of the cross-linker) was observed in the FTIR spectrum (Figure 5). The three-layer PGON-PS-PU system with PGON as a top layer had a thickness of 149 ± 3 nm, indicating that PGON was about 77 nm thick (all layer thickness data were determined by ellipsometry). Optical microscopy and AFM images indicated that the PU layer on the substrate had a mesh-like morphology, possibly due to dewetting from the substrate (see Figure S5 in Section 4 of the Supporting Information).

Disassembly. To disassemble the PGON-PS-PU layer system, it was immersed into NaOH solution for 150 min. Photographs taken after different time intervals document significant changes of the sample appearance (Figure 6), with gas evolution at the edges starting at about 60 min, gas bubble formation in the middle of the sample after 120 min, and visible delamination of the top layer at 140 min. In this experiment, the top layer ruptured and could not be obtained as a whole piece. Overall, PU in the PGON-PS-PU system seemed to depolymerize more slowly than in the PS-PU system. In the FTIR spectrum taken after depolymerization, the peaks at 1706 cm^{-1} (carbonyl signal from PGON), 1531 cm^{-1} (amine signal from PGON), and 1223 cm^{-1} (amide signal from PU) all vanished. The spectrum also contained a sig-

nal at 1063 cm^{-1} which can be assigned to the C–O single bond of the depolymerization product of PU, 4-aminobenzyl alcohol, indicating that traces of delamination product of the former PU layer remained on the substrate.

2.2.5. PZI-PU-PZI Layer System

The PU layers used in the above-described systems were inhomogeneous and mesh-like. To obtain thicker, more homogeneous layers, the spin-coating conditions for PU were adjusted, resulting in discrete layers with a thickness of up to 300 nm. Since the successful disassembly of the PGON-PS-PU layer system confirmed the strong interaction of PU with PGON, a different functional polymer was used in all further systems (PZI, Figure 2). Three PZI-PU-PZI layer system were assembled with PZI as top and bottom layers, respectively, and PU interlayers with different thickness (20, 220, and 300 nm, Figure 7a–c). All systems were studied by ellipsometry, FTIR and AFM.

Assembly. Optical micrographs taken during the assembly of the PZI-PU-PZI layer system are shown in Figure 7. The analytical data is summarized in Figure S6 in Section 5 of the Supporting Information. The FTIR spectra obtained for these three systems were similar, showing additional signals of N–H bond in-plane bending vibrations of PU at $1533\text{--}1527 \text{ cm}^{-1}$, in addition to the signals corresponding to PZI.

Disassembly. To disassemble the three-layer PZI-PU-PZI layer system with a 20 nm PU layer, it was immersed into NaOH aqueous solution for 120 min. Just as with the PS-PU system, delamination was observed after roughly 60 min. The substrate thus obtained seemed blank (Figure 7a), and ellipsometry indicated a remnant layer thickness of be 25 ± 1 nm, which is much lower than the layer thickness of the PZI bottom layer measured during assembly (264 ± 3 nm). The FTIR spectra obtained in the process are summarized in Figure S6a, Section 5 of the Supporting Information; the AFM is shown in Figure S7, Section 6 of the Supporting Information. To compare the PZI-PU-PZI systems a) and b), they were both immersed in NaOH for the same length of time, i.e., 120 min. For system a), delamination was already finished after 60 min, and the longer reaction time unfortunately also reduced the layer thickness of PZI of that system due to extraction of its gel content.

The three-layer system PZI-PU-PZI b) with a 220 nm thick PU layer remained stable until the 120th min. No delamination was observed. In the wet state, it could be optically observed that the adhesion between the layers was weakened (buckling). When gently rinsed with water, the loosened upper layer was partially sheared off. Thus, the upper layer, possibly with PU depolymerization products was “exfoliated” macroscopically under external force. The remaining layer thickness was 284 ± 9 nm (similar to the value 280 ± 4 nm for a single layer of PZI), which indicates an almost clean removal of the upper PZI-PU layer. The FTIR spectra taken after degradation (Figure 8 and Figure S8 in Section 7, Supporting Information) showed a strong signal at 1032 cm^{-1} , which can be ascribed to the C–O–C bands from PZI. Based on this retained functional group, we conclude that both PZI-PU-PZI layer system could shed the topmost antimicrobial polymer layer in consequence of sufficiently fast depolymerization, assisted by gas development. Thus, the system with the 20 nm PU

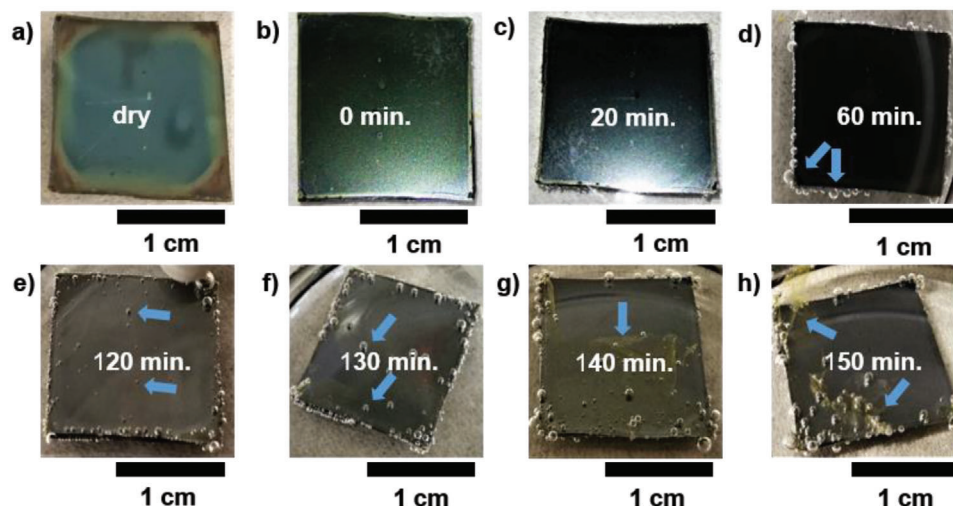


Figure 6. Degradation of the PZON-PS-PU system: a) dry, b) wet, after 0 min, c–h) after 20, 60, 120, 130, 140, and 150 min treatment with NaOH. The blue arrows indicate significant events during the degradation process which are described in the text.

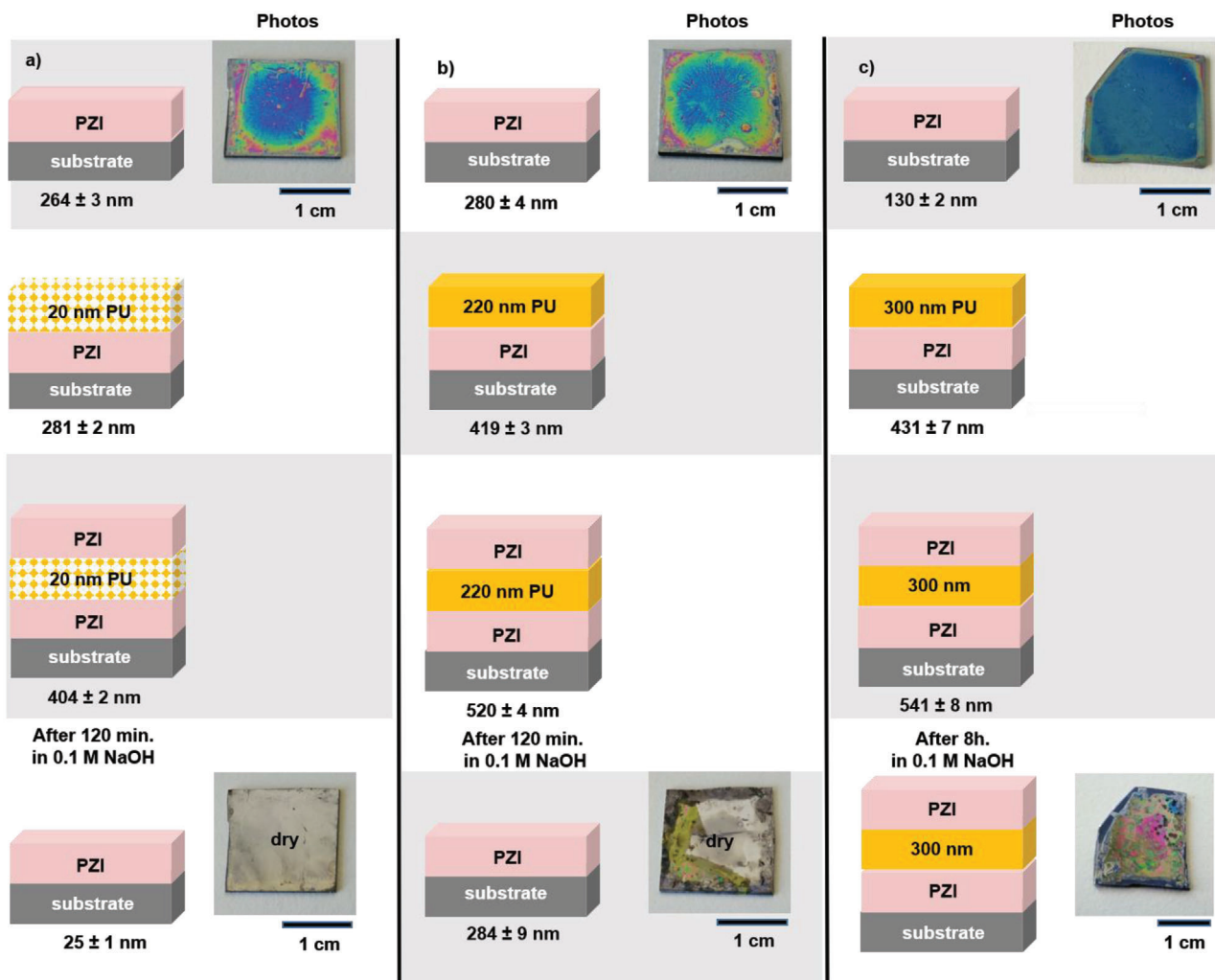


Figure 7. Overview of the design and appearance of the three PZI-PU-PZI stacks during assembly and disassembly. a) PZI-PU-PZI system with a thin PU interlayer between a PZI bottom and top layer, b,c) PZI-PU-PZI layer system with thick PU interlayers.

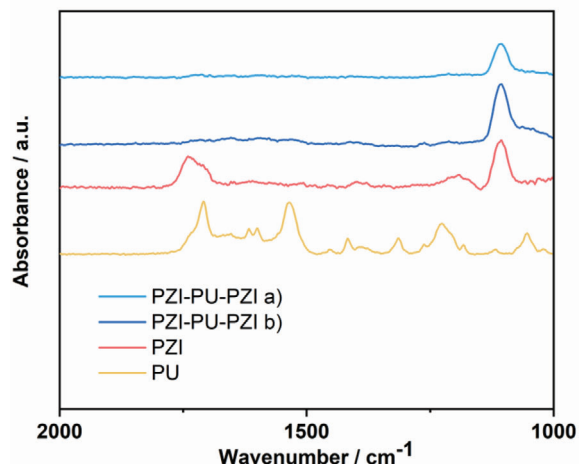


Figure 8. FTIR spectra of the PZI-PU-PZI layer systems with a) 20 nm PU layer and b) 220 nm PU layer after degradation, compared to the spectra of PZI and PU single layers.

layer was self-regenerating, since no additional external force was needed to remove the top functional layer. The system with the 220 nm PU layer needed additional shear forces to enable a complete removal of the top layer.

The PZI-PU-PZI layer system with the 300 nm thick PU layer, system c), was immersed into NaOH aqueous solution for 150 min. The sample was then removed, rinsed, and dried. It was observed that the sample started to peel, and that the coating color changed, thus indicating a change in thickness. To check if longer immersion time would induce further shedding, the sample was placed back into the NaOH solution up to the eighth hour. However, this shedding process did not complete. The thickness of the sample was about 446 ± 9 nm on most of the sample area, which indicates that the top layer was gone and the PU layer and lower PZI layer were still present. In other words, the system with the 300 nm PU layer could not regenerate. The FTIR spectra of the degraded multilayer confirmed this by showing a reduction of the peak intensity by half, while the position of the signals remained mostly the same (Figure S6c in Section 5 of the Supporting Information). The AFM images are shown in Figure S9, Section 8 of the Supporting Information.

3. Discussion

In this work, triggered delamination of polymer layers from a polymer multilayer stack was investigated. Using the PS-PU bilayer system, it was demonstrated that the combined forces arising from mass transport of the degradation products at the layer interfaces, and buoyancy due to gas development within the PU layer during depolymerization were sufficient to delaminate the PS layer. This confirmed the suitability of PU with 2-butanonyl end groups as a sacrificial layer for triggered delamination. However, the strong interactions between PU and the polar, overall positively charged PGON apparently shut down the depolymerization process, i.e., the 1,6-elimination cascade. A similar phenomenon was also observed when poly(adipic anhydride) (PAA) and poly(salicylic-acid-co-sebacic acid) were used as sacrificial layers with PGON as functional layer.^[10] To explain this phe-

nomenon, three possible factors were considered back then: covalent binding between the layers through side reactions with the cross-linker; interdiffusion between the layers due to the slow degradation rate of the sacrificial layer; and third, complexation or more generally, intramolecular interactions between functional and sacrificial layer due to their charges or polarity.^[10b] For the here presented systems, side reactions with the cross-linker can be ruled out, because the cross-linker in PGON and PZI was the same, yet the layer shedding behavior of the two materials was different. Too slow depolymerization can also be excluded, or else the model bilayer system PS-PU should not show delamination. Also, the depolymerization of PU was faster than the degradation of PAA and poly(salicylic-acid-co-sebacic acid) by at least one magnitude. Additionally, PU depolymerization releases CO₂ and thereby prevents reattachment by polymer interdiffusion during degradation. Thus, the ionic interactions between PGON and the sacrificial layers used seem to be responsible for the inability to shed layers from systems involving PGON, unless an uncharged interlayer like PS is used to shield them.

It should be noted that the PU layers fabricated from a mixture of DMF and THF suffered from dewetting and were thus not homogeneous but structured (Figure S5, Supporting Information). The surface roughness was about 102 nm. However, once they were coated with PS and later with PGON, the surface roughness decreased by 67%, and they were of sufficient quality for proof-of-concept.

In the PZI-PU-PZI systems, PU interlayers with three different thicknesses (20, 220, and 300 nm) were used. In the PZI-PU-PZI layer system a) with 20 nm of PU, a rapid and clean delamination was observed, indicating that PZI did not adversely affect the shedding process. When PU was applied onto PZI bottom layer, also from a mixture of DMF and THF, and the average surface roughness was only about 10 nm (Figure S7, Supporting Information). The assembled three-layer system before degradation had an average surface roughness of about 15 nm. This system demonstrated the intended self-regeneration.

For further systems, PU was applied from *N*-methyl pyrrolidone (NMP), which improved the layer quality, i.e., the layer homogeneity. The PZI-PU-PZI layer systems b) with a thicker PU interlayer of 220 nm was assembled to see if thick and homogeneous PU layers have the same potential as the thin and inhomogeneous one to serve as sacrificial layer. The relatively thick PU layer out obtained from NMP had an average surface roughness of 2.3 nm (Figure S8, Supporting Information). The PZI-PU-PZI assembled using this material had an overall surface roughness of 4.6 nm.

When exposed to layer shedding conditions, this multilayer system remained stable for two hours, much longer than the PZI-PU-PZI layer system with the thin layer. Thus, the layer thickness affects the onset of visible depolymerization and layer shedding, possibly due to the time it takes for the aqueous medium to diffuse through the entire layer. While the PU layer also degraded in this system, as demonstrated by FTIR data, delamination of the upper functional layer started only when the sample was subjected to shear forces during rinsing. In the PZI-PU-PZI layer system c) with the thickest PU interlayer of 300 nm, the PU layer seems too thick and too smooth to facilitate delamination of the PZI top layer (roughness of only 0.35 nm according to AFM, see Figure S9, Supporting Information). Thus, there seems to be

strong adhesion between **PU** and **PZI**. In summary, the three-layer **PZI-PU-PZI** system a) and b) can serve as proof-of-concept for triggered layer shedding, in which a functional layer (upper **PZI** layer) is shed and another functional layer (lower **PZI** layer) is revealed.

Another key difference between the depolymerizable **PU** sacrificial layer and the previously reported degradable **PSA**,^[9] poly(adipic anhydride), or poly(salicylic acid-*co*-sebacic acid)^[10a] sacrificial layers, or the water-soluble polymeric sacrificial layers use in microelectronics, is the mechanism of shedding. Both for the degradable and soluble layers, the contact time with the aqueous medium (i.e., the dissolution and degradation kinetics) determine the time point of layer disassembly, i.e., it is a passive process. On the other hand, the depolymerizable **PU** could be stored in aqueous medium at lower pH for a long time without changes to the system, and only the high pH triggered the depolymerization and thus disassembly process. Thus, active triggering is required, which makes surface regeneration on demand accessible.

4. Conclusion and Outlook

In this work, we demonstrated the triggered delamination of a functional layer from polymer multilayer stacks using the self-immolative polymer **PU**, a 4-hydroxy-2-butanonyl end-capped poly(benzyl carbamate), as a sacrificial layer. Its depolymerization can be triggered by alkaline pH of the surrounding medium. With **PU** interlayers, the functional layer of a polymer multilayer stack could be regenerated by immersing the system into aqueous NaOH solution for a certain induction time, which depended on the thickness of the depolymerizable **PU** layer. The crucial factors contributing to the success of layer shedding were the sufficiently fast degradation kinetics of **PU**, and the additional buoyancy force due to gas evolution during depolymerization. In one case, an additional shear force was needed to obtain layer shedding. The data also showed that a variation of the sacrificial layer thickness within a certain range allows to control the shedding/regeneration time-point of the system after exposure to the trigger. By using polymers with triggered depolymerization, it is possible to store the sample in aqueous conditions, and switch on the process by a change of pH.

With further work dedicated into exploring more stimuli-responsive polymers with orthogonal trigger conditions, more sophisticated multilayer stacks capable of sequential shedding and multiple regeneration of functional layers can be envisioned. This kind of self-regenerative system is not limited to the regeneration of the functional surfaces as presented here, but may be applied to other functional surfaces, for example, anti-icing, superhydrophobic, or biosensing surfaces. By shedding the defective or contaminated surface, new functional surfaces emerge, with can prolonged the service life of a device.

5. Experimental Section

Materials: All chemicals used in this work were obtained from Carl Roth (Karlsruhe, Germany), Euriso-Top (Saint Aubin, France), Sigma Aldrich (Munich, Germany), or TCI (Tokyo, Japan), and used as received. Monomers, polymers, and surface functionalization agents were synthe-

sized as described in the literature.^[10b,15–17] Polymer solutions were filtered using CHROMAFIL hydrophilized polytetrafluoroethylene (h-PTFE) syringe filters (pore size 0.2 μm , diameter 13 mm) from Macherey-Nagel (Düren, Germany) prior to application. Silicon substrates were cut into $1.5 \times 1.5 \text{ cm}^2$ pieces from double-side polished silicon wafers ($525 \pm 25 \text{ }\mu\text{m}$ thick standard Si (CZ) wafer with [100] orientation) from Si-Mat (Kaufering, Germany).

Methods: Thickness of polymer films was determined by a multiple angle laser ellipsometer SE400adv from Sentech Instruments (Berlin, Germany). Film morphology was imaged in PeakForce Tapping Mode on a Dimension Icon AFM from Bruker (Billerica, MA, USA). Microscope images was taken using the integrated digital camera with five mega pixels on AFM. FTIR spectra were recorded by a BioRad Excalibur FTS 3000 spectrometer from Varian, Agilent Technologies (Santa Clara, USA). Films were fabricated on a Spin150 wafer spinner from SPS Europe (Putten, Netherlands).

Layer Fabrication: **PS** Layer: 20 mg of polystyrene with 5 mol% of 4-methacryloyloxybenzophenone was dissolved in 1 mL ethyl acetate. The polymer solution was filtered through a syringe filter onto the **PU** surface (coated as described below). The substrates were spun at 3000 rpm with 1000 rpm s^{-1} acceleration for a total of 30 s. The sample was irradiated with UV light (wavelength: 254 nm, energy dose: 3 J cm^{-2}) to form a polymer network.

PGON Layer: Poly(guanidinium oxanorbornene) with 10 mol% of diazoester-functionalized repeat units (**PGON**) was deprotected from their Boc-protecting groups by firstly dissolving the polymer (160 mg) in anhydrous chloroform and later reacting with HCl solution (4 M in dioxane) overnight. To spin-coat **PGON** onto a surface, 10 mg was dissolved in water-methanol mixture (0.02/0.08 mL) as reported in literature.^[10b] The resulted solution after filtering was applied onto the **PU** surface using following parameters: 1000 rpm s^{-1} (acceleration), 3000 rpm (speed), and 10 s (spinning time). The material was UV irradiated (wavelength: 254 nm, energy dose: 0.2 J cm^{-2} for cross-linking).

PZI Layer: The poly(carboxyzwitterion) with 10 mol% of diazoester-functionalized repeat units (**PZI**) was deprotected from their Boc-protecting groups by dissolving the polymer (140 mg) in anhydrous tetrahydrofuran and then reacting with HCl solution (4 M in dioxane) overnight. To spin-coat **PZI** onto surface, 20 mg of freshly deprotected **PZI** was dissolved in 1 mL methanol. Deprotected **PZI** that had been stored in freezer before was dissolved in a water-methanol mixture (0.01/0.09 mL).^[16a] Methanol was probably needed due to substance aging. The filtered **PZI** solution was spin-coated onto the substrate pretreated with 4-[(3-triethoxysilyl)propoxy-benzophenone and 3-aminopropyl triethoxysilane (see Section 2 of the Supporting Information for more detail). The resulting layer was UV irradiated (wavelength: 254 nm, energy dose: 0.1 J cm^{-2}). The energy dose needed was determined by gel content measurement, see Section 9 of the Supporting Information.

PU Layer with 20 nm thickness: 10 mg of **PU** was dissolved in 0.04 mL *N,N*-dimethylformamide. To this solution, 0.78 mL of tetrahydrofuran was added. The polymer solution was applied onto the static substrate through a syringe filter. Sufficient solution was deposited to fully cover the substrate surface. The substrate was then accelerated with 1000 rpm s^{-1} to a final angular speed of 3000 rpm. The total spinning time was 30 s.

PU Layer with 220 nm thickness: 87 mg of **PU** was dissolved in 1 mL 1-methyl-2-pyrrolidone (NMP) at 110 °C. After filtering, the polymer solution was spin-coated onto the respective surfaces for 10 s (3000 rpm, 1000 rpm s^{-1}) and kept on a preheated hotplate at 110 °C for 10 s to avoid dewetting.

PU Layer with 300 nm thickness: 200 mg of **PU** was dissolved in NMP at 110 °C. The coating process was the same as for the layer with 220 nm thickness.

Supporting Information

Supporting Information is available from the Wiley Online Library or from the author.

Acknowledgements

Funding of this project by the European Research Council (grant agreement No.: ERC-StG 637920 Regenerate) is gratefully acknowledged. Natalia Schatz, Esther Riga, and Stefan Paschke are gratefully acknowledged for synthesizing the functional materials polystyrene with 5% cross-linker, poly(guanidium oxanorbornene) with 10% cross-linker and poly(carboxyzwitterion) with 10% cross-linker. The authors thank Dr. Harald Scherer for teaching the procedure of quantitative NMR measurement and Natalia Schatz for measuring gel permeation chromatography samples.

Open access funding enabled and organized by Projekt DEAL.

Conflict of Interest

The authors declare no conflict of interest.

Data Availability Statement

Research data are not shared.

Keywords

coatings, polymer multilayers, polymeric materials, self-regeneration, surface modification, triggered depolymerization

Received: April 15, 2021

Revised: July 23, 2021

Published online: September 13, 2021

- [1] M. F. Montemor, *Surf. Coat. Technol.* **2014**, 258, 17.
- [2] a) S. Pletincx, L. L. I. Fockaert, J. M. C. Mol, T. Hauffman, H. Terryn, *npj Mater. Degrad.* **2019**, 3, 23; b) G. Grundmeier, M. Stratmann, *Annu. Rev. Mater. Res.* **2005**, 35, 571.
- [3] V. M. Shkolnikov, *Hybrid Ship Hulls: Engineering Design Rationales*, Elsevier Science, New York, USA **2014**.
- [4] a) C. Coupeau, *Mater. Sci. Eng., A* **2008**, 483–484, 617; b) J. Carroll, S. Xia, A. M. Beese, R. B. Berke, G. J. Pataky, *Fracture, Fatigue, Failure and Damage Evolution, Volume 7: Proceedings of the 2017 Annual Conference on Experimental and Applied Mechanics*, Springer International Publishing, **2017**.
- [5] a) S. O. Ojo, S. O. Ismail, M. Paggi, H. N. Dhakal, H. N. Dhakal, *Composites, Part B* **2017**, 124, 207; b) J. Jokinen, M. Kanerva, *Appl. Compos. Mater.* **2019**, 26, 709.
- [6] a) L. Alibardi, *Zoology (Jena)* **2009**, 112, 403; b) L. Alibardi, *J. Morphol.* **2015**, 276, 144; c) T. Okano, N. Yamada, H. Sakai, Y. Sakurai, *J. Biomed. Mater. Res.* **1993**, 27, 1243; d) T. Okano, N. Yamada, M. Okuhara, H. Sakai, Y. Sakurai, in *The Biomaterials: Silver Jubilee Compendium* (Ed.: D. F. Williams), Elsevier Science, Oxford, **1995** pp. 109–115; e) S. Sekiya, T. Shimizu, M. Yamato, A. Kikuchi, T. Okano, *Biochem. Biophys. Res. Commun.* **2006**, 341, 573; f) J. Yang, M. Yamato, C. Kohno, A. Nishimoto, H. Sekine, F. Fukai, T. Okano, *Biomaterials* **2005**, 26, 6415; g) A. K. A. S. Brun-Graepi, C. Richard, M. Bessodes, D. Scherman, O.-W. Merten, *Prog. Polym. Sci.* **2010**, 35, 1311; h) O. Guillaume-Gentil, M. Gabi, M. Zenobi-Wong, J. Vörös, *Biomed. Microdevices* **2011**, 13, 221.
- [7] F. Dorner, A. Malek-Luz, J. S. Saar, S. Bonaus, A. Al-Ahmad, K. Lienkamp, *Macromol. Chem. Phys.* **2016**, 217, 2154.
- [8] S. S. Ono, G. Decher, *Nano Lett.* **2006**, 6, 592.
- [9] F. Dorner, D. Boschert, A. Schneider, W. Hartleb, A. Al-Ahmad, K. Lienkamp, *ACS Macro Lett.* **2015**, 4, 1337.
- [10] a) Z. Deng, E. K. Riga, K. Lienkamp, *Macromol. Chem. Phys.* **2020**, 221, 2000106; b) E. K. Riga, E. Gillies, K. Lienkamp, *Adv. Mater. Interfaces* **2019**, 6, 1802049.
- [11] a) H. Zhang, Y. Liu, C. Yang, L. i Xiang, Y. Hu, L.-M. Peng, *Adv. Mater.* **2018**, 30, 1805408; b) J. G. Ibanez, A. Alatorre-Ordaz, S. Gutierrez-Granados, N. Batina, *Polym. Degrad. Stab.* **2008**, 93, 827.
- [12] A. Sagi, R. Weinstain, N. Karton, D. Shabat, *J. Am. Chem. Soc.* **2008**, 130, 5434.
- [13] A. M. Dilauro, H. Zhang, M. S. Baker, F. Wong, A. Sen, S. T. Phillips, *Macromolecules* **2013**, 46, 7257.
- [14] G. Liu, X. Wang, J. Hu, G. Zhang, S. Liu, *J. Am. Chem. Soc.* **2014**, 136, 7492.
- [15] a) G. J. Gabriel, A. E. Madkour, J. M. Dabkowski, C. F. Nelson, K. Nüsslein, G. N. Tew, *Biomacromolecules* **2008**, 9, 2980; b) E. K. Riga, Dissertation, University of Freiburg, April, 2018.
- [16] a) M. Kurowska, A. Eickenscheidt, D. -. L. Guevara-Solarte, V. T. Widyaya, F. Marx, A. Al-Ahmad, K. Lienkamp, *Biomacromolecules* **2017**, 18, 1373; b) M. Hess, R. G. Jones, J. Kahovec, T. Kitayama, P. Kratochvíl, P. Kubisa, W. Mormann, R. F. T. Stepto, D. Tabak, J. Vohlídal, E. S. Wilks, *Pure Appl. Chem.* **2006**, 78, 2067; c) S. Paschke, K. Lienkamp, *ACS Appl. Polym. Mater.* **2020**, 2, 129.
- [17] B. Berchtold, Dissertation, University of Freiburg, September, 2005; b) E. K. Riga, J. Rühle, K. Lienkamp, *Macromol. Chem. Phys.* **2018**, 219, 1800397.
- [18] G. Socrates, *Infrared and Raman Characteristic Group Frequencies: Tables and Charts*, Wiley, Chichester, UK **2004**.
- [19] a) K. Kikuchi, S. N. Thorn, D. Hilvert, *J. Am. Chem. Soc.* **1996**, 118, 8184; b) F. Hollfelder, A. J. Kirby, D. S. Tawfik, *Nature* **1996**, 383, 60; c) R. P. Taylor, *J. Am. Chem. Soc.* **1976**, 98, 2684.